NO_3 chemistry of wildfire emissions: a kinetic study of the gas-phase reactions of furans with the NO_3 radical

Mike J. Newland, Yangang Ren, Max R. McGillen, Lisa Michelat, Véronique Daële, Abdelwahid Mellouki

ICARE-CNRS, 1 C Av. de la Recherche Scientifique, 45071 Orléans Cedex 2, France

Correspondence to: Mike J. Newland (mike.newland@cnrs-orleans.fr); Abdelwahid Mellouki (mellouki@cnrs-orleans.fr)

Abstract. Furans are emitted to the atmosphere during biomass burning from the pyrolysis of cellulose. They are one of the major contributing VOC classes to OH and NO_3 reactivity in biomass burning plumes. The major removal process of furans from the atmosphere at night is reaction with the nitrate radical, NO_3. Here we report a series of relative rate experiments in the 7300 L indoor simulation chamber at CNRS-ICARE, Orléans, using a number of different reference compounds to determine NO_3 reaction rate coefficients for four furans, two furanones, and pyrrole. In the case of the two furanones, this is the first time that NO_3 rate coefficients have been reported. The recommended values (cm^3 $molecule^{-1}$ s^{-1}) are: furan $(1.49\pm0.23)\times10^{-12}$, 2-methylfuran $(2.26\pm0.52)\times10^{-11}$, 2,5-dimethylfuran $(1.02\pm0.31)\times10^{-10}$, furfural (furan-2-aldehyde) $(9.07\pm2.3)\times10^{-14}$, α-angelicalactone (5-methyl-2(3H)-furanone) $(3.01\pm0.45)\times10^{-12}$, γ-crotonolactone (2(5H)-furanone) $<1.4\times10^{-16}$, and pyrrole $(6.94\pm1.9)\times10^{-11}$. The furfural + NO_3 reaction rate coefficient is found to be an order of magnitude smaller than previously reported. These experiments show that for furan, alkyl substituted furans, α-angelicalactone, and pyrrole, reaction with NO_3 will be the dominant removal process at night, and may also contribute during the day. For γ-crotonolactone, reaction with NO_3 is not an important atmospheric sink.

1 Introduction

Furans are five membered aromatic cyclic ethers. Furans (and pyrroles – where N replaces O as the heteroatom) are generated during the pyrolysis of cellulose and are a major component of emissions from wildfire burning (Hatch et al., 2015, 2017; Koss et al., 2018; Coggon et al., 2019; Andreae et al., 2019). Such emissions are likely to increase in the future with the spatial extent, number, and severity, of wildfires globally having increased markedly in recent decades (Jolly et al., 2015; Harvey, 2016) and predicted to continue to do so as the climate warms (Krikken et al., 2019; Lohmander, 2020). Furans have also been measured in emissions from residential logwood burning (Hartikainen et al., 2018), and burning of a wide variety of solid-fuels used for domestic heating and cooking (Stewart et al., 2021a). Furans have been shown to account for a significant proportion of the total NO_3 (Decker et al., 2019) and OH (Koss et al., 2018; Coggon et al., 2019; Stewart et al., 2021b) reactivity of emissions from burning of typical wildfire and domestic fuels.

Alkyl substituted furans have also been suggested as promising biofuels as they can be derived from lignocellulosic biomass (Roman-Leshkov et al., 2007; Binder et al., 2009; Wang et al., 2014). This would likely lead to fugitive emissions of these compounds during distribution, as well as emissions of unburned and partially oxidised products from vehicle exhaust. The oxidation of certain furan compounds has been shown to have large secondary organic aerosol yields (Hatch et al., 2017; Hartikainen et al., 2018; Joo et al., 2019, Ahern et al., 2019; Akherati et al., 2020), which could adversely impact air quality.

Oxidation of furans in the atmosphere has been shown to produce 2-furanones (mono-unsaturated five-membered cyclic esters) both via OH (notably hydroxy-furan-2-ones, Aschmann et al., 2014) and NO_3 (Berndt et al., 1997) reactions. 2-Furanones are

also produced from the OH oxidation of six-membered aromatic compounds (Smith et al., 1998, 1999; Hamilton et al., 2005; Bloss et al., 2005; Wyche et al., 2009; Huang et al., 2015). In both cases, the initial product is thought to be an unsaturated dicarbonyl, with production of the 2-furanone formed via photoisomerisation of the dicarbonyl to a ketene-enol (Newland et al., 2019), followed by ring closure of this molecule. In the case of aromatics, the ketene-enol can also be formed directly via decomposition of the bicyclic peroxy radical intermediate (Wang et al., 2020).

Furan type compounds are removed from the atmosphere by reaction with the major oxidants OH, NO_3 and O_3. There have been a number of studies on the rates of reaction of furan type compounds with the dominant daytime oxidant, OH (Lee and Tang, 1982; Atkinson et al., 1983; Wine and Thompson, 1984; Bierbach et al., 1992, 1994, 1995; Aschmann et al., 2011; Ausmeel et al., 2017; Whelan et al., 2020). However, there have been fewer studies on the rates of reaction of furan type compounds with the major night-time oxidant, NO_3 (Atkinson et al., 1985; Kind et al., 1996; Cabañas et al., 2004; Colmenar et al., 2012).

The nitrate radical, NO_3, is produced in the atmosphere predominantly through the reaction of NO_2 with O_3, and exists in equilibrium with N_2O_5. It has long been known to be an important night-time oxidant (Levy, 1972; Winer et al., 1984). While it is also produced during the daytime, it is rapidly converted back to NO_2 by reaction with NO and by photolysis. However, in environments with low NO, either due to low NOx emissions, or suppression through high O_3 concentrations (e.g. Newland et al., 2021), NO_3 oxidation has been observed to be significant during the day (Hamilton et al., 2021).

Here, we present results of a series of relative rate experiments for furan, 2-methylfuran, 2,5-dimethylfuran, furfural (furan-2-aldehyde), α-angelicalactone (5-methyl-2(3H)-furanone), γ-crotonolactone (2(5H)-furanone), and pyrrole reaction with the NO_3 radical, performed in the 7300 L indoor simulation chamber at CNRS-ICARE, Orléans, France.

2 Experimental

2.1 CSA-Chamber

The CNRS-ICARE indoor chamber is a 7300 L indoor simulation chamber used for studying reaction kinetics and mechanisms under atmospheric boundary layer conditions. Further details of the chamber setup and instrumentation are available elsewhere (Zhou et al., 2017). Experiments were performed in the dark at atmospheric pressure (*ca.* 1000 mbar), with the chamber operated at a slight overpressure to compensate for removal of air for sampling, and to prevent ingress of outside air to the chamber. The chamber is in a climate controlled room and the temperature was maintained at 299±2 K.

2.2 Experimental Approach

Starting with the chamber filled with clean air, the VOCs of interest (*ca*. 3 ppmv) were added, followed by ~ 1 Torr of the inert gas SF_6 to monitor the chamber dilution rate. A flow of 5 L/min of purified air was continuously added throughout the experiment, and air is then removed from the chamber to maintain a constant pressure (this is a slight overpressure to prevent possible ingress of air from outside the chamber). The chamber was left for at least thirty minutes prior to the start of the experiment to monitor the dilution rate and losses of the VOCs to the chamber walls. These losses, $(1 - 8)\times10^{-6}$ s^{-1}, were always smaller than dilution ($\sim1.2\times10^{-5}$ s^{-1}). The reaction was then initiated by continuously introducing an N_2O_5 sample, held in a trap at ~ 235 K with a part of the purified air flow (2.5 – 5) L/min directed through it, for the duration of the experiment. The chamber was monitored until

most of the VOC of interest was consumed, with experiments generally taking 0.5 – 2 hours. The experiments were performed under dry conditions (RH ≤ 1.5 %).

VOC abundance was determined by *in-situ* Fourier Transform Infrared (FTIR) Spectroscopy using a Nicolet 5700 coupled to a White-type multipass cell with a pathlength of 143 m. Each scan was comprised of either 30 or 60 co-additions, taking a total of 2 or 4 minutes respectively, depending on the expected rate of loss of the VOCs, with a spectral resolution of 0.25 cm^{-1}.

2.3 Materials

The VOCs of interest: furan (>99%, Sigma-Aldrich), 2-methylfuran (>98%, TCI), 2,5-dimethylfuran (>98%, TCI), pyrrole (>99%, TCI), α-angelicalactone (>98%, TCI), furfural (>98%, TCI), and γ-crotonolactone (>93%, TCI); and reference compounds: 2,3-dimethyl-but-2-ene (98%, Sigma-Aldrich), 2-carene (97%, Sigma-Aldrich), camphene (95%, Sigma-Aldrich), α-pinene (98%, Sigma-Aldrich), cyclohexene (≥99%, Sigma-Aldrich), 3-methyl-3-buten-1-ol (97%, Sigma-Aldrich), and cyclohexane (99.5%, Sigma-Aldrich), were used as supplied without further purification.

N_2O_5 was synthesised by reacting NO_2 with excess O_3. First, NO and O_3 were mixed to generate NO_2 (Reaction R1). This NO_2 / O_3 mixture was then flushed into a bulb in which NO_3 and subsequently N_2O_5 were generated through Reactions R2-R3.

$NO + O_3 \rightarrow NO_2$ (R1)

$NO_2 + O_3 \rightarrow NO_3$ (R2)

$NO_2 + NO_3 \rightarrow N_2O_5$ (R3)

N_2O_5 crystals were then collected in a cold trap at 190K. The N_2O_5 sample was purified by trap to trap distillation under a flow of O_2 / O_3. The final sample was stored at 190 K and used within a week.

2.4 Analysis

VOC concentrations were monitored by FTIR. The furans generally have a number of major absorption bands in the infrared. The main bands used for analysis are shown in Table 1 (bold), as well as other characteristic bands for each compound. Reference spectra of the major bands for each compound taken in the chamber at a resolution of 0.25 cm^{-1} are provided in the Supplement (Figures S8-S14). The ANIR curve fitting software (Ródenas, 2018), which implements a least squares fitting algorithm was used to generate time profiles for each compound based on their reference spectra. Profiles were checked by doing a number of manual subtractions. Example time profiles from an experiment with α-angelicalactone and furan, with cyclohexene as the reference compound, are shown in Figure 1. Further example plots are provided in the supplement (Figures S1-S7). All of the concentration-time profiles are provided in .txt format at 10.5281/zenodo.5721518, and all the raw FTIR output is provided in .csv format at 10.5281/zenodo.5721518. Relative rate plots for all of the experiments are shown in Figure 2.

Table 1 Maxima of major absorption bands (of Q branches if present) for the compounds used in this study. Bands used predominantly for analysis are shown in bold.

Compound	Main absorption bands / cm^{-1}
Furan	**995**, 744
2-Methylfuran	**792**, 726, 1151, 2965
2,5-Dimethylfuran	**777**, 2938, 2961
Furfural	**756**, 1720
Pyrrole	**724**, 1017, 3531, 718-722
α-angelicalactone	**731, 939**, 1100, 1834
γ-crotonolactone	**1098,** 805, 866, 1045, 1812, 2885, 2945
2,3-Dimethyl-2-butene	**2878, 2930, 3005**
2-Carene	**2874, 2928, 3009**
α-pinene	**2971, 2998, 3035,** 789, 2847, 2893, 2925, 2931
Camphene	**2967, 2972, 2986**, 882, 2881, 3075
Cyclohexene	**2934,** 744, 919, 1140, 2892, 2943, 3033, 3036
3-Methyl-3-buten-1-ol	**1065,** 896, 903, 2886, 2948, 2981, 3084
Cyclohexane	**2862, 2933**

Relative rate experiments were performed, whereby a compound (or two) with an unknown reaction rate coefficient (k_{VOC}) with NO_3 was added to the chamber with a reference compound with a known NO_3 reaction rate coefficient (k_{ref}). A plot of the relative loss of the compound against the reference compound following addition of NO_3 (via N_2O_5 decomposition), accounting for both chamber dilution and wall losses (k_d), gives a gradient of k_{VOC}/k_{ref} (Equation E1).

$$\ln\frac{([VOC]_0)}{([VOC]_t)} - k_d t = \frac{k_{VOC}}{k_{ref}} \ln\frac{[ref]_0}{[ref]_t} - k_d t \qquad \text{(E1)}$$

A number of reference compounds were used for each VOC, chosen so that the reference rate coefficient was roughly within a factor of five of the expected unknown rate coefficient, and with an attempt to use different references that had both larger and smaller NO_3 reaction rate coefficients than the VOC. Rate coefficients of the reference compounds (Table 2) are taken from the Database for the Kinetics of the Gas-Phase Atmospheric Reactions of Organic Compounds v2.1.0 (McGillen et al., 2020), available at data.eurochamp.org/data-access/kin/#/home.

N_2O_5 was not present at detectable levels (by FTIR) during most of the experiments. The only experiments in which N_2O_5 concentrations built up in the chamber, were those with the slowest reacting VOCs, i.e. furfural and γ-crotonolactone. NO_2 concentrations increased throughout all experiments, typically up to 2 – 3 ppmv. The NO_2 is initially produced from the decomposition of N_2O_5, and later potentially by the loss of NO_2 from nitrated VOCs / nitrated radicals. HNO_3 concentrations

increased throughout the experiments, typically up to 3 – 4 ppmv. This could be either due to impurities in the N_2O_5 sample, or from H abstraction reactions of NO_3. It is not thought that this level of HNO_3 will cause any interference in the rate coefficient determinations.

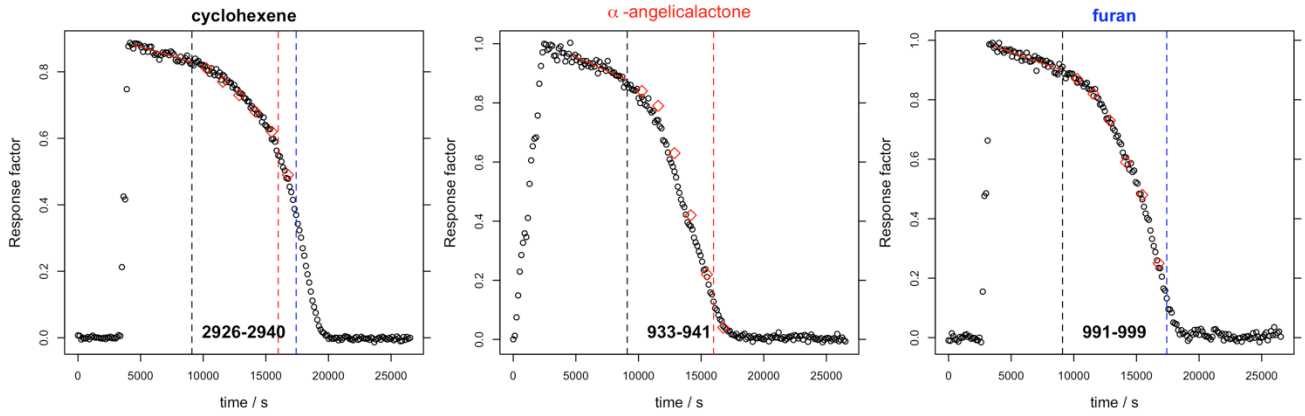

Figure 1 Concentration-time profiles from experiment with cyclohexene, α-angelicalactone and furan. Black circles are response factors generated by the ANIR curve fitting program relative to the reference spectra. Red diamonds are obtained from manual subtractions. Left black dashed vertical line is the beginning of the region used for the relative rate calculation, the red dashed line is the end of the region used for the calculation of the α-angelicalactone relative rate, the blue line is the end of the region used for the calculation of the furan relative rate. Bold values at the bottom are the absorption bands used for analysis.

Table 2. Reference compounds used. Recommended rate coefficients and uncertainties from McGillen et al. (2020).

Compound	***k* / cm^3 molecule^{-1} s^{-1}**
2,3-dimethyl-2-butene	$(5.70\pm1.71)\times10^{-11}$
2-carene	$(2.0\pm0.3)\times10^{-11}$
α-pinene	$(6.20\pm1.55)\times10^{-12}$
camphene	$(6.60\pm1.65)\times10^{-13}$
cyclohexene	$(5.60\pm0.84)\times10^{-13}$
3-methyl-3-buten-1-ol	$(2.60\pm0.78)\times10^{-13}$
cyclohexane	$(1.35\pm0.20)\times10^{-16}$

It is noted that no OH scavenger was used in these experiments (as is the case for most, if not all, NO_3 previous relative rate studies to the authors' knowledge). NO_3 reaction with alkenes tends to proceed by electrophilic addition to the double bond followed by addition of O_2 to the resulting radical, leading to a nitrooxy peroxy radical (β-ONO_2-RO_2) (Barnes et al., 1989; Hjorth et al., 1990). It has recently been shown (Novelli et al., 2021) that there is the possibility of OH formation through the reactions of β-ONO_2-RO_2 with HO_2. HO_2 could be generated in these experiments from the abstraction of an H atom by O_2 from a β-ONO_2-RO radical with available H atoms. The initial NO_3 reaction with furans is not thought to form β-ONO_2-RO_2 radicals, with NO_3 addition to the C2 carbon followed by O_2 addition to the C_5 carbon (Berndt et al., 1997), analogous to the OH addition reaction (Bierbach et al., 1995; Mousavipour et al., 2009; Yuan et al., 2017; Whelan et al., 2020). However, some of the reference compounds used in the experiments will form such radicals. For example, the reaction of HO_2 with the β-ONO_2-RO_2 radicals

formed from α-pinene + NO_3 has been reported to have an OH yield of up to 70 % (Kurtén et al., 2017). An additional minor source of HO_2 during the experiments will be H abstraction reactions by NO_3. These will produce RO_2 that can react to form RO radicals which may yield HO_2 following abstraction of an H atom by O_2. However, the rate coefficient of H abstraction by NO_3 is generally expected to be negligible relative to that of the NO_3 addition pathway. A box model run was performed to test the impact of this chemistry in this study. The α-pinene scheme from the MCMv3.3.1 (Jenkin et al., 1997; mcm.york.ac.uk) was incorporated into the box model AtChem (Sommariva et al., 2020), and an OH yield of 0.5 was assigned to the reaction of HO_2 with the initial β-ONO_2-RO_2 radicals formed from the α-pinene+NO_3 reaction. The model was initiated with 2-methylfuran and α-pinene concentrations of 3 ppmv, representative of the experiments performed here. NO_3 concentrations were constrained to give a lifetime of ~ 1 hour for the VOCs, typical of the experiments. OH reaction was found to account for less than 1 % of the removal of 2-methylfuran or α-pinene through the model run. Consequently, it can be assumed that OH chemistry is a negligible interference in these experiments.

A further potential interference with the current experimental setup, is the reaction of NO_2 with the compounds used. Rate coefficients have been measured for reaction of NO_2 with a number of unsaturated compounds (Atkinson et al., 1984; Bernard et al., 2013). For conjugated dienes, these values can be large enough (~10^{-18} cm^3 $molecule^{-1}$ s^{-1}) to provide a significant loss under the experimental conditions employed here. NO_2 is formed during these experiments from the decomposition of N_2O_5, with the NO_2 mixing ratio typically increasing up to roughly 3 ppmv through the experiment. Separate experiments were performed to look at the potential reaction of NO_2 with furan, 2,5-dimethylfuran and pyrrole. The experiments were performed with initial VOC mixing ratios of 3 ppmv, and initial NO_2 mixing ratios of roughly 5 ppmv, similar to the maximum amount of NO_2 observed during the NO_3 experiments. For all three compounds, their loss in the presence of NO_2 (allowing for dilution) was indistinguishable from zero, allowing an upper limit of < 2×10^{-20} cm^3 $molecule^{-1}$ s^{-1} to be placed on their $k(NO_2)$ rate coefficients. Based on these experiments, it was assumed that the $k(NO_2)$ rate coefficients for 2-methylfuran, furfural, and a-angelicalactone are likely to be of a similar magnitude, and hence provide negligible interference under the experimental conditions employed.

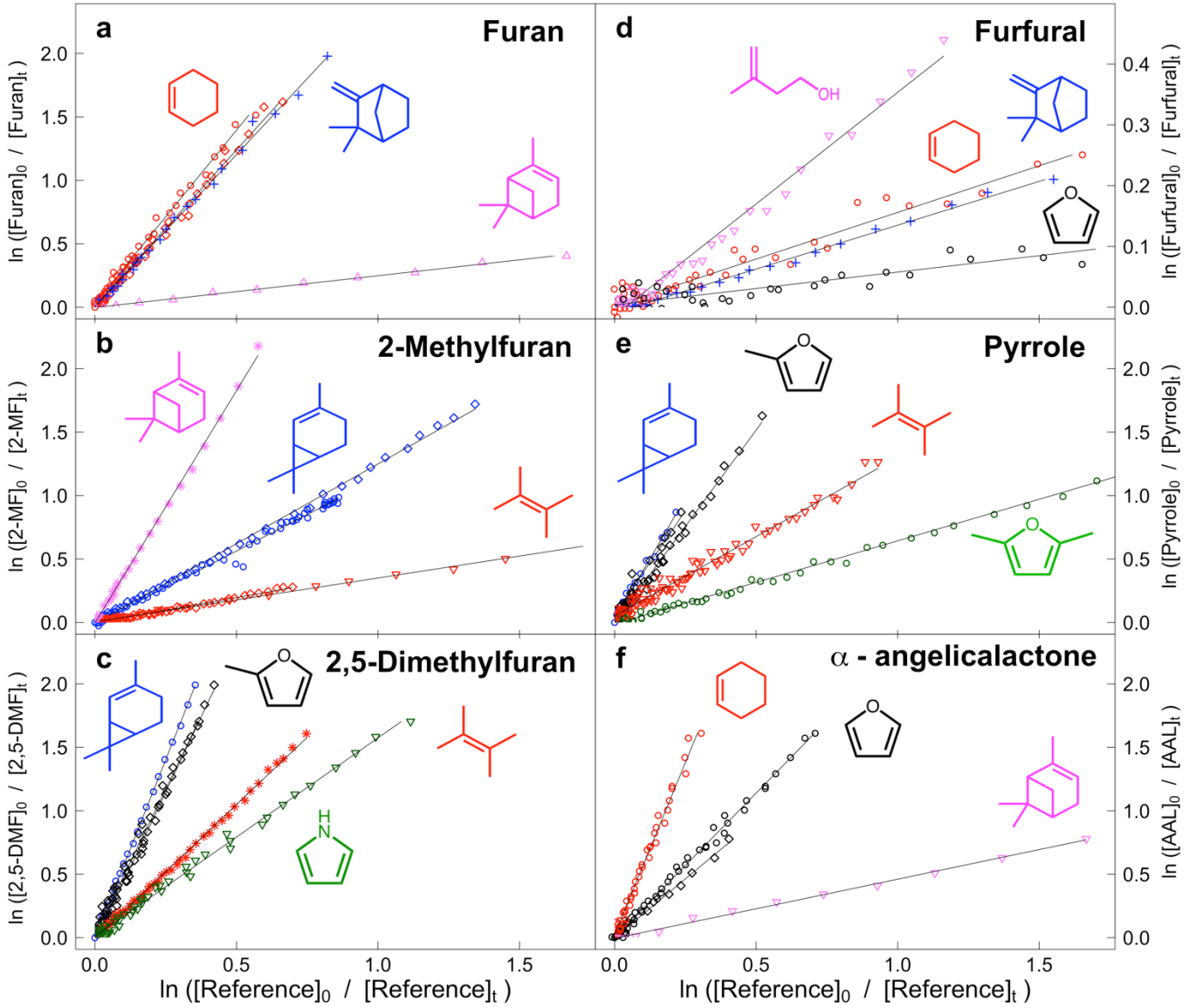

Figure 2. Relative rate plots for: **a.** furan relative to cyclohexene (red), camphene (blue), and α-pinene (pink); **b.** 2-methylfuran relative to 2-carene (blue), 2,3-dimethyl-2-butene (red), and α-pinene (pink); **c.** 2,5-dimethylfuran relative to 2-carene (blue), 2,3-dimethyl-2-butene (red), 2-methylfuran (black), and pyrrole (green); **d.** furfural relative to camphene (blue), cyclohexene (red), furan (black), and 3-methyl-3-buten-1-ol (pink); **e.** pyrrole relative to 2-carene (blue), 2,3-dimethyl-2-butene (red), 2-methylfuran (black), and 2,5-dimethylfuran (green); **f.** α-angelicalactone relative to cyclohexene (red), furan (black), and α-pinene (pink). Different shapes are used for different experiments with the same reference compound.

3 Results and Discussion

The $k(NO_3)$ rate coefficients determined with each reference compound are given in Table 3 and Figure 3. Overall recommended values for the rate coefficient for each compound are calculated by taking the mean (weighted by the reported uncertainty of the reference) of the rate coefficient derived from each experiment with each reference compound, including using the recommended values for the other furans presented in Table 3. Uncertainties for the relative rates in Table S1 are assumed to be < 10 % and to

be dominated by statistical errors in fitting to the absorption bands. Uncertainties for the rate coefficients reported in Table 3 are dominated by the assumed uncertainties in $k(NO_3)$ of the reference compounds. For most of the references, the uncertainties are 20 – 30 %, taken from the recommendations of McGillen et al. (2020). For 2,3-dimethyl-2-butene, the recommended uncertainty in McGillen et al. (2020) is 150 %, but based on the fact that the rate coefficients derived using 2,3-dimethyl-2-butene for 2-methylfuran, 2,5-dimethylfuran and pyrrole agree very well with those using other references with much smaller uncertainties, a conservative estimate of 30 % is used here. It is noted that for all compounds, the rate coefficients derived with different references agree very well, to within 10%. The experimentally determined $k(NO_3)$ rate coefficients of the furans relative to each other are in good agreement (to within 6%) with those calculated using the weighted means shown in Table 3 (Table S2). This gives further confidence in the $k(NO_3)$ values used for the reference compounds.

The rate coefficient derived for furan, agrees well with the value previously reported by Atkinson et al. (1985) from a chamber relative rate experiment. However, there is significant differences between the values reported here for furan, 2-methylfuran and 2,5-dimethylfuran, and those reported by Kind et al. (1996) from relative rate experiments in a flow reactor. While the value reported for 2-methylfuran agrees within the uncertainties between the two studies, the values for furan and 2,5-dimethylfuran reported here are ~ 50 % and 100 % greater respectively. It is unclear what is behind this observed disparity; the good agreement between the two studies for the 2-methylfuran rate coefficient suggests that there is not a systematic difference between the experimental setups. For pyrrole, the rate coefficient determined here is about 50% faster than the value reported by Atkinson et al. (1985) from a chamber relative rate experiment using N_2O_5 thermal decomposition. Cabañas et al. (2004) reported an upper limit of $<1.8\times10^{-10}$ cm^3 molecule^{-1} s^{-1} (298K) using an absolute technique of fast flow discharge.

For 2-furanaldehyde (furfural) + NO_3, the rate coefficient recommended here is an order of magnitude slower than the only previously reported values (Colmenar et al., 2012), derived from small chamber relative rate experiments with 2-methyl-2-butene and α-pinene as references. The rate coefficient from Colmenar et al. (2012) is very similar to the reported rate coefficient for furan+NO_3. This is surprising, since the presence of a formyl group attached to a double bond is expected to be strongly deactivating with respect to addition to that bond, due to the electron withdrawing mesomeric effect of the –C(O)H group (Kerdouci et al., 2014). This has also been observed for other electrophilic addition reactions, such as those with OH and O_3 (Kwok and Atkinson, 1995; McGillen et al, 2011; Jenkin et al., 2020). And while there is the possibility of H abstraction from the formyl group, which would increase the overall rate coefficient, such reactions are typically of the order of 10^{-14} cm^{3}s^{-1} (Kerdouci et al., 2014), and hence would not be expected to compensate for the reduction in the contribution to the overall rate coefficient of the addition reaction.

For 5-methyl-(3H)-furan-2-one (α-angelica lactone) + NO_3 this is the first reported rate coefficient. For (5H)-furan-2-one (γ-crotonolactone), relative rate experiments with several reference compounds were attempted, with the slowest reacting of these being cyclohexane ($k_{NO3} = 1.4\times10^{-16}$ cm^3 molecule^{-1} s^{-1}). In this experiment, roughly 10 % of the cyclohexane was removed by reaction with NO_3 (accounting for loss by dilution), whereas there was no appreciable chemical loss of γ-crotonolactone. We can therefore deduce that k(γ-crotonolactone+NO_3) $<< 1.4\times10^{-16}$ cm^3 molecule^{-1} s^{-1}. Again, this is the first time a NO_3 reaction rate coefficient has been measured for this compound. A comparison of the two furanones shows that 5-methyl-(3H)-furan-2-one reacts more than four orders of magnitude faster than (5H)-furan-2-one. This can be explained in part by the presence of a methyl group, which is seen to increase the rate coefficient by roughly an order of magnitude from e.g. furan to 2-methylfuran to 2,5-dimethylfuran. Berndt et al. (1997) derived an NO_3 reaction rate coefficient of 1.76×10^{-13} cm^3 molecule^{-1} s^{-1} for (3H)-furan-2-

one. However, the majority of the difference must be explained by the structure of the two compounds, namely the conjugated nature of the C=C and C=O bonds in (5H)-furan-2-one. The carbonyl group removes electron density from the C=C bond greatly reducing the rate coefficient. A similar relationship is seen for analogous acyclic compounds e.g. the NO_3 rate coefficient of the conjugated ester methyl acrylate is almost two orders of magnitude greater than that of the non-conjugated isomer vinyl acetate.

Table 3. NO_3 reaction rate coefficients derived for each experiment and recommended value based on the weighted mean.

Compound	Reference (repeats)	$k(NO_3)$ / cm^3 $molecule^{-1}$ s^{-1}	Weighted mean $k(NO_3)$ / cm^3 $molecule^{-1}$ s^{-1}
2,5-dimethylfuran 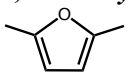	2-carene (1)	1.12×10^{-10}	**$1.02\pm0.31\times10^{-10}$**
	2,3-dimethyl-2-butene (1)	1.21×10^{-10}	
	pyrrole (1)	9.12×10^{-11}	
	2-methylfuran (2)	9.06×10^{-11}	
pyrrole 	2-carene (1)	7.68×10^{-11}	**$6.94\pm1.9\times10^{-11}$**
	2,3-dimethyl-2-butene (2)	7.07×10^{-11}	
	2,5-dimethylfuran (1)	6.58×10^{-11}	
	2-methylfuran (2)	6.37×10^{-11}	
2-methylfuran 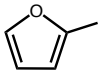	2-carene (3)	2.47×10^{-11}	**$2.26\pm0.52\times10^{-11}$**
	2,3-dimethyl-2-butene (2)	2.12×10^{-11}	
	α-pinene (1)	2.27×10^{-11}	
	pyrrole (2)	1.89×10^{-11}	
	2,5-dimethylfuran (2)	2.21×10^{-11}	
α-angelicalactone 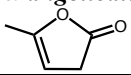	α-pinene (1)	2.89×10^{-12}	**$3.01\pm0.45\times10^{-12}$**
	cyclohexene (1)	3.03×10^{-12}	
	furan (2)	3.05×10^{-12}	
furan 	cyclohexene (1)	1.45×10^{-12}	**$1.49\pm0.23\times10^{-12}$**
	α-pinene (1)	1.55×10^{-12}	
	camphene (1)	1.58×10^{-12}	
	α-angelicalactone (2)	1.49×10^{-12}	
furfural 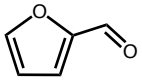	cyclohexene (1)	8.57×10^{-14}	**$9.07\pm2.30\times10^{-14}$**
	3-methyl-3-buten-1-ol (1)	9.54×10^{-14}	
	furan	8.37×10^{-14}	
	camphene (1)	9.50×10^{-14}	
γ-crotonolactone 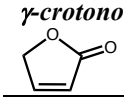	cyclohexane (1)	$< 1.4\times10^{-16}$	**$< 1.4\times10^{-16}$**

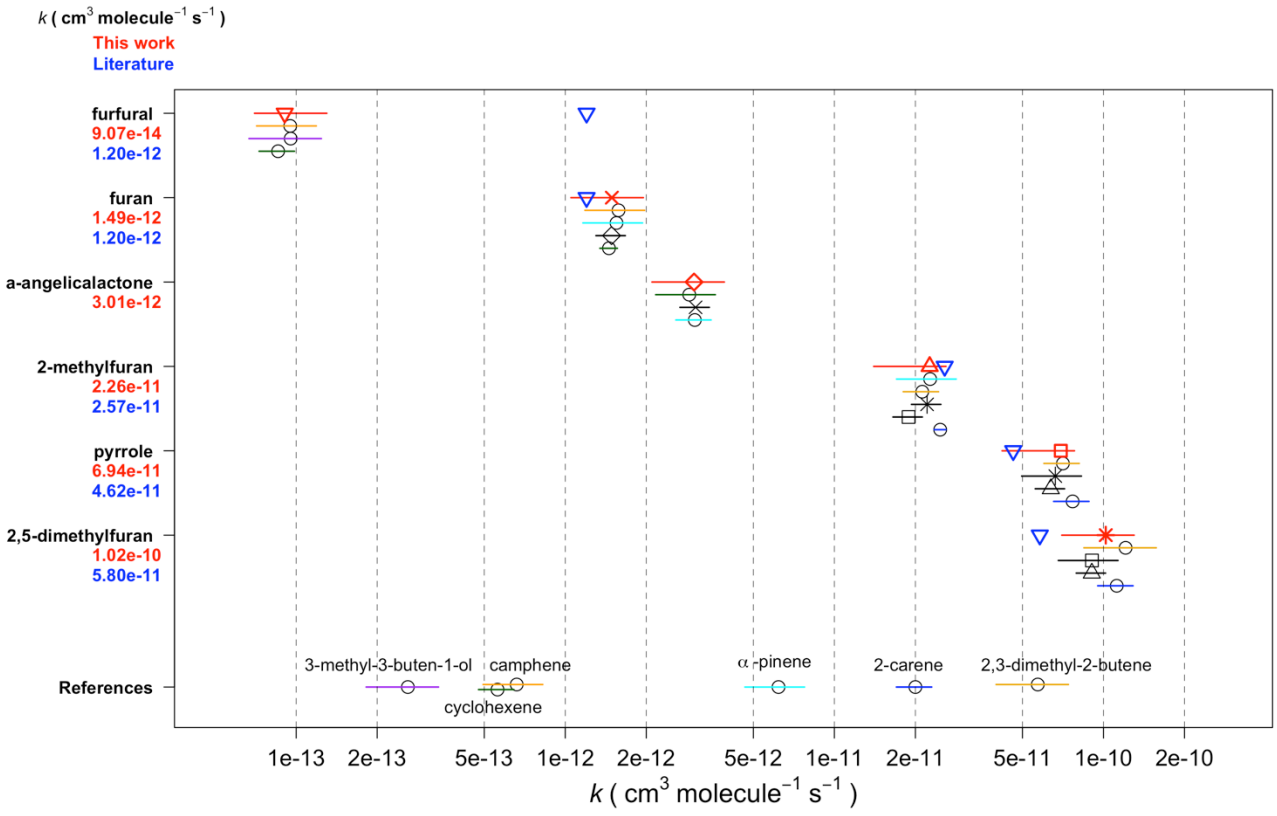

Figure 3 The reaction rate coefficients derived for the six compounds in this work (excluding γ-crotonolactone). Red triangles (and red text, left axis) represent the weighted mean of all experiments in this work, blue inverted triangles (and blue text, left axis) are the recommended values from McGillen et al. (2020). Horizontal lines represent uncertainty in rate coefficient, colours (shapes if other furans) represent which reference was used.

Table 4. Recommended NO_3 rate coefficients from this work compared to those reported in the literature.

Compound	Rate coefficient / cm^3 $molecule^{-1}$ s^{-1}	Reference	Technique	NO_3 source
2,5-dimethylfuran	**$(1.02\pm0.31)\times10^{-10}$**	**This work**		
	$(5.78\pm0.34)\times10^{-11}$	Kind et al. (1996)	Flow reactor: relative (*trans*-2-butene)	N_2O_5
pyrrole	**$(6.94\pm1.9)\times10^{-11}$**	**This work**		
	$(4.6\pm1.1)\times10^{-11}$	Atkinson et al. (1985)	Chamber: relative (2-methyl-2-butene)	N_2O_5
	$< 1\times10^{-10}$	Cabañas et al. (2004)	Flow reactor: absolute (LIF detection of NO_3)	HNO_3+F
2-methylfuran	**$(2.26\pm0.52)\times10^{-11}$**	**This work**		
	$(2.57\pm0.17)\times10^{-11}$	Kind et al. (1996)	Flow reactor: relative (*trans*-2-butene)	N_2O_5
α-*angelicalactone*	**$(3.01\pm0.45)\times10^{-12}$**	**This work**		
furan	**$(1.49\pm0.23)\times10^{-12}$**	**This work**		
	$(1.5\pm0.2)\times10^{-12}$ [b]	Atkinson et al. (1985)	Chamber: relative (*trans*-2-butene)	N_2O_5
	$(0.998\pm0.062)\times10^{-12}$	Kind et al. (1996)	Flow reactor: relative (*trans*-2-butene)	N_2O_5
	$(1.36\pm0.8)\times10^{-12}$	Cabañas et al. (2004)	Flow reactor: absolute (LIF detection of NO_3)	HNO_3+F

furfural	**(9.07±2.30)×10^{-14}**	**This work**		
	(1.17±0.15)×10^{-12}	Colmenar et al. (2012)	Small chamber: relative (2-methyl-2-butene)	N_2O_5
	(1.36±0.38)×10^{-12}	Colmenar et al. (2012)	Small chamber: relative (α-pinene)	N_2O_5
γ-crotonolactone	**< 1.4×10^{-16}**	**This work**		

[a] corrected for change to recommended rate for reference (2,3-dimethyl-2-butene); [b] corrected for change to recommended rate for reference (trans-2-butene)

4 Atmospheric implications

The atmospheric lifetimes of the compounds, based on the rate coefficients reported herein, are given in Table 5. These assume concentrations of OH = 5×10^6 molecules cm^{-3} (typical daily peak summertime concentrations 1.5×10^6 – 1.5×10^7 molecules cm^{-3} (Stone et al., 2012)), night-time NO_3 = 2×10^8 molecules cm^{-3} (typical night-time concentrations 1×10^8 – >1×10^9 cm^{-3} (Brown and Stutz (2012)) daytime NO_3 = 1×10^7 molecules cm^{-3} (limited daytime measurements suggest concentrations ~ 0.5 – >1 pptv (2.5×10^7 molecules cm^{-3}) (Brown and Stutz (2012)), and O_3 = 40 ppbv (background O_3 concentration ~ 40 ppb (Parrish et al., 2014)). It is noted that oxidant concentrations have a high spatial and temporal variability due to variability in their sources and sinks, and that oxidant levels within biomass burning plumes in particular are poorly understood. Hence the relative importance of the oxidants shown in Table 5 is likely to vary dependent on conditions. From the values given in Table 5, it is clear that the alkyl substituted furans and pyrrole have very short lifetimes both during the day, when the dominant daytime sink is likely to be reaction with OH, and at night, when the dominant sink will be reaction with NO_3. O_3 may contribute somewhat to the removal of these compounds both during the day and night, particularly for 2,5-dimethylfuran. As $k(NO_3)$ approaches the same order of magnitude as k(OH), e.g. for 2-methylfuran, 2,5-dimethylfuran and pyrrole, the NO_3 reaction is likely to be competitive with the OH reaction even during the day in low NOx environments, with daytime NO_3 concentrations reported to be ~ 1 ppt (2.5×10^7 molecules cm^{-3}) (Brown and Stutz, 2012). The relatively large rate coefficient reported here for α-angelicalactone, suggests that NO_3 reaction will be an important sink for unsaturated non-conjugated cyclic esters. On the other hand, the very small rate coefficient for the γ-crotonolactone +NO_3 reaction suggests that this will not be an important atmospheric sink. γ-crotonolactone has also been shown to have a very slow reaction with O_3 (lifetime > 100 years, Ausmeel et al., 2017), whereas for reaction with OH, the lifetime is much shorter, and this will be the predominant gas-phase sink for γ-crotonolactone . Such a slow NO_3 reaction might be expected to extend to all 2-furanones with a conjugated structure, e.g. hydroxyfuranones – major products of OH oxidation of methyl substituted furans (Aschmann et al., 2014), such that the nitrate reaction may be unimportant in the atmosphere for these structures. Although substitution at the double bond is likely to increase the rate coefficient somewhat, as observed for OH and O_3 reactions with the methyl-substituted form of γ-crotonolactone (Ausmeel et al., 2017).

One of the major sources of furan type compounds to the atmosphere is wildfires. Wildfire plumes can be regions of high NO_3 even during the day due to suppressed photolysis rates in optically thick plumes (Decker et al, 2021). NO_3 oxidation of furans may be even more important in such plumes than in the background atmosphere. Such plumes can extend over hundreds of kilometres and hence affect air quality on a local and regional scale (e.g. Andreae et al., 1988; Brocchi et al., 2018; Johnson et al., 2021). Domestic wood burning is an increasing trend in northern European cities (Chafe et al., 2015). Burning will generally be in the winter during which, with short daylight hours and peak daytime OH often an order of magnitude lower than during the summer, the reaction with NO_3 is likely to be the dominant fate of furan type compounds in such emissions, contributing significantly to organic aerosol in urban areas (Kodros et al., 2020).

Berndt et al. (1997) identified the major first generation products of furan+NO_3 to be the unsaturated dicarbonyl, butenedial, and 2(3H)-furanone, with the NO_3 recycled back to NO_2. However, Tapia et al. (2011), and Joo et al. (2019) found that the major products of the 3-methylfuran+NO_3 reaction predominantly retain the NO_3 functionality. In this case, furan+NO_3 oxidation chemistry may be a significant sink for NOx, sequestering it in nitrate species, which might release it far from source on further gas-phase oxidation, or, due to their low volatility, be taken up into aerosol (Joo et al. 2019).

Table 5. Atmospheric gas-phase lifetimes of the compounds reported herein based on typical mid-day OH concentrations of 5×10^6 molecules cm^{-3}, night-time NO_3 concentrations of 2×10^8 molecules cm^{-3}, day-time NO_3 concentrations of 1×10^7 molecules cm^{-3}, and background O_3 concentrations of 40 ppbv (1×10^{12} molecules cm^{-3}).

Compound	$\tau_{NO3\ (night)}$	$\tau_{NO3\ (day)}$	$\tau_{OH\ (day)}$	τ_{O3}	$\tau_{total\ (day)}$
2,5-dimethylfuran	0.82 min	16 min	26 min [a]	40 min [b]	8 min
2-methylfuran	3.7 min	74 min	48 min [a]	-	28 min
furan	56 min	19 hours	83 min [a]	116 hours [c]	77 min
pyrrole	1.2 min	24 min	28 min [d]	18 hours [d]	13 mins
furfural	15 hours	13 days	95 min [e]	-	94 min
α-angelicalactone	28 min	9.3 hours	48 min [f]	3.5 hours [g]	37 mins
γ-crotonolactone	> 1.1 year	> 22 years	14 hours [h]	173 years	14 hours

[a] Matsumoto (2011); [b] Dillon et al. (2012); [c] Atkinson et al. (1983); [d] Atkinson et al. (1984); [e] Bierbach et al. (1995); [f] Bierbach et al. (1994); [g] estimated (Bierbach et al., 1994); [h] Ausmeel et al. (2017)

5 Conclusions

Rate coefficients are recommended for reaction of seven furan type VOCs with NO_3 at 298 K and 760 Torr, based on a series of relative rate experiments. These new recommendations highlight the importance of NO_3 chemistry to the removal of furans, and other similar VOCs, under atmospheric conditions. The measured rate coefficients suggest that for the three furans reported here, as well as for pyrrole and α-angelicalactone, reaction with NO_3 is likely to be their dominant night-time sink. For the alkyl furans

and pyrrole, reaction with NO_3 may also be a significant sink during the daytime. This work also extends the existing database of VOC+NO_3 reactions, providing valuable reference values for future work.

Data availability. Further example plots and experiment information are provided in the supplement. All of the response-time profiles from the FTIR are provided in .txt format at 10.5281/zenodo.5724967, and all of the raw FTIR output is provided in .csv format at 10.5281/zenodo.5721518.

Author contributions. MJN performed the experiments with the technical support of YR and MRM and performed the data treatment and interpretation. MJN wrote the paper. All co-authors revised the content of the original manuscript and approved the final version of the paper.

Competing interests.

The authors declare that they have no conflict of interest.

Special issue statement. This article is part of the special issue "Simulation chambers as tools in atmospheric research (AMT/ACP/GMD inter-journal SI)". It is not associated with a conference.

Acknowledgements.

This work is supported by the European Union's Horizon 2020 research and innovation program through the EUROCHAMP-2020 Infrastructure Activity under grant agreement no. 730997, Labex Voltaire (ANR-10-LABX-100-01) and ANR (SEA_M project, ANR-16-CE01-0013, program ANR-RGC 2016).

Financial support. This research has been supported by the European Commission Horizon 2020 Framework Programme (grant no. EUROCHAMP-2020 (730997)) and the Agence Nationale de la Recherche (grants nos. ANR-10-LABX-100-01 and ANR-16-CE01-0013)

References

Ahern, A. T., Robinson, E. S., Tkacik, D. S., Saleh, R., Hatch, L. E., Barsanti, K. C., Stockwell, C. E., Yokelson, R. J., Presto, A. A., Robinson, A. L., Sullivan, R. C., and Donahue, N. M.: Production of Secondary Organic Aerosol During Aging of Biomass Burning Smoke From Fresh Fuels and Its Relationship to VOC Precursors, J. Geophys. Res.-Atmos., 124, 3583–3606, 2019.

Akherati, A., He, Y., Coggon, M. M., Koss, A. R., Hodshire, A. L., Sekimoto, K., Warneke, C., de Gouw, J., Yee, L., Seinfeld, J. H., Onasch, T. B., Herndon, S. C., Knighton, W. B., Cappa, C. D., Kleeman, M. J., Lim, C. Y., Kroll, J. H., Pierce, J. R., and Jathar, S. H.: Oxygenated Aromatic Compounds are Important Precursors of Secondary Organic Aerosol in Biomass Burning Emissions, Environ. Sci. Technol., 54, 8568–8579, https://doi.org/10.1021/acs.est.0c01345, 2020.

Andreae, M. O., Browell, E. V., Garstang, M,. Gregory, G. L., Harriss, R. C., Hill, G. F., Jacob, D. J., Pereira, C., Sachse, G. W., Setzer, A. W., Silva Dias, P. L., Talbot, R. W., Torres, A. L., and Wofsy, S. C.: Biomass-burning emissions and associated haze layers over Amazonia, J. Geophys. Res.-Atmos, 93, 1509-1527, 1988.

Andreae, M. O.: Emission of trace gases and aerosols from biomass burning – an updated assessment, Atmos. Chem. Phys., 19, 8523–8546, https://doi.org/10.5194/acp-19-8523-2019, 2019.

Aschmann, S. M., Nishino, N., Arey J., and Atkinson, R.: Products of the OH radical-initiated reactions of furan, 2- and 3-methylfuran, and 2,3- and 2,5-dimethylfuran in the presence of NO, J. Phys. Chem. A, 118, 457-466, 2014.

Atkinson, R., Aschmann, S. M., and Carter, W. P. L.: Kinetics of the reactions of O3 and OH radicals with furan and thiophene at 298 +/- 2 K, Int. J. Chem. Kinet., 15, 51-61, 1983.

Atkinson, R., Aschmann, S. M., Winer, A. M., and Carter, W. P. L.: Rate Constants for the Gas Phase Reactions of OH Radicals and O_3 with Pyrrole at 295 +/- 1 K and Atmospheric Pressure, Atmos. Environ., 18, 2105-2107, 1984.

Atkinson, R., Aschmann, S. M., Winer, A. M., and Pitts, J. N.: Gas-phase reactions of NO_2 with alkenes and dialkenes, Int. J. Chem. Kinet., 16, 697-706, 1984.

Atkinson, R., Aschmann, S. M., Winer, A. M., and Carter, W. P. L.: Rate Constants for the Gas Phase Reactions of NO_3 Radicals with Furan, Thiophene and Pyrrole at 295 +/- 1 K and Atmospheric Pressure, Environ. Sci. Technol., 19, 87-90, 1985.

Ausmeel, S., Andersen, C., Nielsen, O. J., Østerstrøm, F. F., Johnson, M. S., and Nilsson, E. J. K.: Reactions of Three Lactones with Cl, OD, and O_3: Atmospheric Impact and Trends in Furan Reactivity, J. Phys. Chem. A, 121, 4123-4131, 2017.

Barnes, I., Bastian, V., Becker, K. H., and Tong, Z.: Kinetics and products of the reactions of nitrate radical with monoalkenes, dialkenes, and monoterpenes, J. Phys. Chem., 94, 2413–2419, 1990.

Bernard, F., Cazaunau, M., Mu, Y., Wang, X., Daële, V,. Chen, J., and Mellouki, A.: Reaction of NO_2 with conjugated alkenes, J. Phys. Chem. A, 117, 14132-14140, 2013.

Berndt, T., Böge, O., and Rolle, W.: Products of the Gas-Phase Reactions of NO_3 Radicals with Furan and Tetramethylfuran, Environ. Sci. Technol., 31, 1157–1162, 1997.

Bierbach, A., Barnes, I., Becker, K. H., and Wiesen, E.: Atmospheric Chemistry of Unsaturated Carbonyls: Butenedial, 4-Oxo-2-pentenal, 3-Hexene-2,5-dione, Maleic Anhydride, 3H-Furan-2-one, and 5-Methyl-3H-furan-2-one, Environ. Sci. Technol., 28, 715-729, 1994.

Bierbach, A., Barnes, I., and Becker, K. H.: Product and kinetic study of the OH-initiated gas-phase oxidation of furan, 2-methylfuran and furanaldehydes at ≈ 300 K, Atmos. Environ., 29, 2651–2660, 1995.

Binder, J. B., and Raines, R. T.: Simple Chemical Transformation of Lignocellulosic Biomass into Furans for Fuels and Chemicals. J. Am. Chem. Soc., 131, 1979−1985, 2009.

Bloss, C., Wagner, V., Jenkin, M. E., Volkamer, R., Bloss, W. J., Lee, J. D., Heard, D. E., Wirtz, K., Martin-Reviejo, M., Rea, G., Wenger, J. C., and Pilling, M. J.: Development of a detailed chemical mechanism (MCMv3.1) for the atmospheric oxidation of aromatic hydrocarbons, Atmos. Chem. Phys., 5, 641–664, https://doi.org/10.5194/acp-5-641-2005, 2005.

Brocchi, V., Krysztofiak, G., Catoire, V., Guth, J., Marécal, V., Zbinden, R., El Amraoui, L., Dulac, F., and Ricaud, P.: Intercontinental transport of biomass burning pollutants over the Mediterranean Basin during the summer 2014 ChArMEx-GLAM airborne campaign, Atmos. Chem. Phys., 18, pp. 6887-6906, 2018.

Brown, S., and Stutz, J.: Nighttime radical observations and chemistry, Chem. Soc. Rev., 41, 6405-6447, 2012.

Cabañas, B., Baeza, M. T., Salgado, S., Martín, P., Taccone, R., and Martínez, E.: Oxidation of heterocycles in the atmosphere: Kinetic study of their reactions with NO_3 radical, J. Phys. Chem. A, 108, 10818-10823, 2004.

Chafe, Z., Brauer, M., Héroux, M. –E., Klimont, Z., Lanki, T., Salonen, R. O., and Smith, K. R.: Residential heating with wood and coal: health impacts and policy options in Europe and North America, WHO Regional Office for Europe. https://apps.who.int/iris/handle/10665/153671, 2015.

Coggon, M. M., Lim, C. Y., Koss, A. R., Sekimoto, K., Yuan, B., Gilman, J. B., Hagan, D. H., Selimovic, V., Zarzana, K. J., Brown, S. S., M Roberts, J., Müller, M., Yokelson, R., Wisthaler, A., Krechmer, J. E., Jimenez, J. L., Cappa, C., Kroll, J. H., De Gouw, J. and Warneke, C.: OH chemistry of non-methane organic gases (NMOGs) emitted from laboratory and ambient biomass burning smoke: Evaluating the influence of furans and oxygenated aromatics on ozone and secondary NMOG formation, Atmos. Chem. Phys., 19, 14875–14899, doi:10.5194/acp-19-14875-2019, 2019.

Colmenar, I., Cabañas, B., Martínez, E., Salgado, M. S., and Martín, P.: Atmospheric fate of a series of furanaldehydes by their NO_3 reactions, Atmos. Environ., 54, 177-184, 2012.

Decker, Z. C. J., Zarzana, K. J., Coggon, M., Min, K.-E., Pollack, I., Ryerson, T. B., Peischl, J., Edwards, P., Dubé, W. P., Markovic, M. Z., Roberts, J. M., Veres, P. R., Graus, M., Warneke, C., de Gouw, J., Hatch, L. E., Barsanti, K. C. and Brown, S. S.: Nighttime Chemical Transformation in Biomass Burning Plumes: A Box Model Analysis Initialized with Aircraft Observations, Environ. Sci. Technol., 53, 2529–2538, doi:10.1021/acs.est.8b05359, 2019.

Dillon, T. J., Tucceri, M. E., Dulitz, K., Horowitz, A., Vereecken, L., and Crowley, J.: Reaction of Hydroxyl Radicals with C4H5N (Pyrrole): Temperature and Pressure Dependent Rate Coefficients, J. Phys. Chem. A, 116, 6051-6058, 2012.

Harvey B. J.: Human-caused climate change is now a key driver of forest fire activity in the western United States, Proc. Natl. Acad. Sci., 113, 11649-11650*,* 2016.

Hartikainen, A., Yli-Pirilä, P., Tiitta, P., Leskinen, A., Kortelainen, M., Orasche, J., Schnelle-Kreis, J., Lehtinen, K., Zimmermann, R., Jokiniemi, J., and Sippula, O.: Volatile Organic Compounds from Logwood Combustion: Emissions and Transformation under Dark and Photochemical Aging Conditions in a Smog Chamber, Environ. Sci. Technol., 52, 4979-4988, 2018.

Hatch, L. E., Luo, W., Pankow, J. F., Yokelson, R. J., Stockwell, C. E., and Barsanti, K. C.: Identification and quantification of gaseous organic compounds emitted from biomass burning using two-dimensional gas chromatography–time-of-flight mass spectrometry, Atmos. Chem. Phys., 15, 1865–1899, https://doi.org/10.5194/acp-15-1865-2015, 2015.

Hatch, L. E., Yokelson, R. J., Stockwell, C. E., Veres, P. R., Simpson, I. J., Blake, D. R., Orlando, J. J., and Barsanti, K. C.: Multi-instrument comparison and compilation of non-methane organic gas emissions from biomass burning and implications for smoke-derived secondary organic aerosol precursors, Atmos. Chem. Phys., 17, 1471–1489, 2017.

Hjorth, J., Lohse, C., Nielsen, C. J., Skov, H., and Restelli, G.: Products and mechanism of the gas-phase reaction between NO_3 and a series of alkenes, J. Phys. Chem., 94, 7494–7500, 1990.

Jenkin, M. E., Saunders, S. M., and Pilling, M. J.: The tropospheric degradation of volatile organic compounds: a protocol for mechanism development, Atmos. Environ., 31, 81–104, https://doi.org/10.1016/S1352-2310(96)00105-7, 1997 (data available at: http://mcm.york.ac.uk, last access: 12 August 2021).

Jenkin, M. E., Valorso, R., Aumont, B., Newland, M. J., and Rickard, A. R.: Estimation of rate coefficients for the reactions of O_3 with unsaturated organic compounds for use in automated mechanism construction, Atmos. Chem. Phys., 20, 12921–12937, https://doi.org/10.5194/acp-20-12921-2020, 2020.

Johnson, M. S., Strawbridge, K., Knowland, K. E., Keller, C., and Travis, M.: Long-range transport of Siberian biomass burning emissions to North America during FIREX-AQ, Atmos. Environ., 252, 118241, 2021

Jolly, W. M., Cochrane, M. A., Freeborn, P. H., Holden, Z. A., Brown, T. J., Williamson, G. J., and Bowman, D. M. J. S.: Climate-induced variations in global wildfire danger from 1979 to 2013, Nat. Commun., 6, 7537, 2015.

Kerdouci, J., Picquet-Varrault, B., and Doussin, J. –F.: Structure activity relationship for the gas-phase reactions of NO_3 radical with organic compounds: Update and extension to aldehydes, Atmos. Environ., 84, 363-372, 2014.

Kind, I., Berndt, T., Böge, O., and Rolle, W.: Gas-phase rate constants for the reaction of NO_3 radicals with furan and methyl-substituted furans, Chem. Phys. Lett., 256, 679-683, 1996.

Kodros, J., Papanastasiou, D., Paglione, M., Masiol, M. and Squizzato, S.: Rapid dark aging of biomass burning as an overlooked source of oxidized organic aerosol, 117, 33028-33033, 2020.

Koss, A. R., Sekimoto, K., Gilman, J. B., Selimovic, V., Coggon, M. M., Zarzana, K. J., Yuan, B., Lerner, B. M., Brown, S. S., Jimenez, J. L., Krechmer, J., Roberts, J. M., Warneke, C., Yokelson, R. J., and de Gouw, J.: Non-methane organic gas emissions from biomass burning: identification, quantification, and emission factors from PTR-ToF during the FIREX 2016 laboratory experiment, Atmos. Chem. Phys., 18, 3299–3319, https://doi.org/10.5194/acp-18-3299-2018, 2018.

Krikken, F., Lehner, F., Haustein, K., Drobyshev, I., and van Oldenborgh, G. J.: Attribution of the role of climate change in the forest fires in Sweden 2018, Nat. Hazards Earth Syst. Sci., 21, 2169–2179, https://doi.org/10.5194/nhess-21-2169-2021, 2021.

Kurtén, T., Møller, K. H., Nguyen, T. B., Schwantes, R. H., Misztal, P. K., Su, L., Wennberg, P. O., Fry J. L., and Kjaergaard, H. G.: Alkoxy Radical Bond Scissions Explain the Anomalously Low Secondary Organic Aerosol and Organonitrate Yields From alpha-Pinene + NO_3, J. Phys. Chem. Lett., 8, 2826–2834, 2017.

Kwok, E. S. C., and Atkinson, R.: Estimation of hydroxyl radical reaction rate constants for gas-phase organic compounds using a structure-reactivity relationship: An update, Atmos. Environ., 29, 1685-1695, 10.1016/1352-2310(95)00069-b, 1995.

Lohmander, P.: Forest fire expansion under global warming conditions: Multivariate estimation, function properties, and predictions for 29 countries, Central Asian Journal of Environmental Science and Technology Innovation, 5, 262-276, 2020.

Matsumoto, J.: Kinetics of the reactions of ozone with 2,5-dimethylfuran and its atmospheric implications, Chem. Lett., 40, 582-583, 2011.

McGillen, M. R., Archibald, A. T., Carey, T., Leather, K. E., Shallcross, D. E., Wenger, J. C., and Percival, C. J.: Structure-activity relationship (SAR) for the prediction of gas-phase ozonolysis rate coefficients: an extension towards heteroatomic unsaturated species, Phys. Chem. Chem. Phys., 13, 2842-2849, 2011.

McGillen, M. R., Carter, W. P. L., Mellouki, A., Orlando, J. J., Picquet-Varrault, B., and Wallington, T. J.: Database for the kinetics of the gas-phase atmospheric reactions of organic compounds, Earth Syst. Sci. Data, 12, 1203–1216, https://doi.org/10.5194/essd-12-1203-2020, 2020.

Newland, M. J., Rea, G. J., Thüner, L. P., Henderson, A. P., Golding, B. T., Rickard, A. R., Barnes, I., and Wenger, J.: Photochemistry of 2-butenedial and 4-oxo-2-pentenal under atmospheric boundary layer conditions, Phys. Chem. Chem. Phys., 21, 1160-1171, 2019.

Novelli, A., Cho, C., Fuchs, H., Hofzumahaus, A., Rohrer, F., Tillmann, R., Kiendler-Scharr, A., Wahner, A., and Vereecken, L.: Experimental and theoretical study on the impact of a nitrate group on the chemistry of alkoxy radicals, 23, 5474-5495, 2021.

Parrish, D. D., Lamarque, J. F., Naik, V., Horowitz, L., Shindell, D. T., Staehelin, J., Derwent, R., Cooper, O. R., Tanimoto, H., Volz-Thomas, A., Gilge, S., Scheel, H. E., Steinbacher, M. and Fröhlich, M.: Long-term changes in lower tropospheric baseline ozone concentrations: Comparing chemistry-climate models and observations at northern midlatitudes, J. Geophys. Res., 119, 5719–5736, doi:10.1002/2013JD021435, 2014.

Ródenas, M: software for analysis of Infrared spectra. EUROCHAMP-2020 project, 2018. Available at https://data.eurochamp.org/anasoft

Roman-Leshkov, Y., Barrett, C. J., Liu, Z. Y., and Dumesic, J. A.: Production of Dimethylfuran for Liquid Fuels from Biomass-derived Carbohydrates, Nature, 447, 982−985, 2007.

Smith, D. F., McIver, C. D., and Kleindienst, T. E.: Primary product distribution from the reaction of hydroxyl radicals with toluene at ppb NOx mixing ratios, J. Atmos. Chem., 30, 209–228, 1998.

Smith, D. F., Kleindienst, T. E., and McIver, C. D.: Primary Product Distributions from the Reaction of OH with m-, p-Xylene, 1,2,4- and 1,3,5-Trimethylbenzene, J. Atmos. Chem., 34, 339–364, 1999.

Sommariva, R., Cox, S., Martin, C., Borońska, K., Young, J., Jimack, P. K., Pilling, M. J., Matthaios, V. N., Nelson, B. S., Newland, M. J., Panagi, M., Bloss, W. J., Monks, P. S., and Rickard, A. R.: AtChem (version 1), an open-source box model for the Master Chemical Mechanism, Geosci. Model Dev., 13, 169–183, https://doi.org/10.5194/gmd-13-169-2020, 2020.

Stewart, G. J., Acton, W. J. F., Nelson, B. S., Vaughan, A. R., Hopkins, J. R., Arya, R., Mondal, A., Jangirh, R., Ahlawat, S., Yadav, L., Sharma, S. K., Dunmore, R. E., Yunus, S. S. M., Hewitt, C. N., Nemitz, E., Mullinger, N., Gadi, R., Sahu, L. K., Tripathi, N., Rickard, A. R., Lee, J. D., Mandal, T. K., and Hamilton, J. F.: Emissions of non-methane volatile organic compounds from combustion of domestic fuels in Delhi, India, Atmos. Chem. Phys., 21, 2383–2406, https://doi.org/10.5194/acp-21-2383-2021, 2021a.

Stewart, G. J., Nelson, B. S., Acton, W. J. F., Vaughan, A. R., Hopkins, J. R., Yunus, S. S. M., Hewitt, C. N., Nemitz, E., Mullinger, N., Gadi, R., Rickard, A. R., Lee, J. D., Mandal, T. K., and Hamilton, J. F.: Comprehensive organic emission profiles, secondary organic aerosol production potential, and OH reactivity of domestic fuel combustion in Delhi, India, Environ. Sci.: Atmos., https://doi.org/10.1039/D0EA00009D, online first, 2021b.

Stone, D., Whalley, L., and Heard, D.: Tropospheric OH and HO_2 radicals: field measurements and model comparisons, Chem. Soc. Rev., 41, 6348-6404, 2012.

Wang, J. J., Liu, X. H., Hu, B. C., Lu, G. Z., Wang, Y. Q.: Efficient Catalytic Conversion of Lignocellulosic Biomass into Renewable Liquid Biofuels via Furan Derivatives. RSC Adv., 4, 31101− 31107, 2014.

Whelan, C. A., Eble, J. Mir, Z. S., Blitz, M. A., Seakins, P. W., Olzmann, M., and Stone D.: Kinetics of the Reactions of Hydroxyl Radicals with Furan and Its Alkylated Derivatives 2-Methyl Furan and 2,5-Dimethyl Furan, *J. Phys. Chem. A*, 124, 7416–7426, 2020.

Wyche, K. P., Monks, P. S., Ellis, A. M., Cordell, R. L., Parker, A. E., Whyte, C., Metzger, A., Dommen, J., Duplissy, J., Prevot, A. S. H., Baltensperger, U., Rickard, A. R., and Wulfert, F.: Gas phase precursors to anthropogenic secondary organic aerosol: detailed observations of 1,3,5-trimethylbenzene photooxidation, Atmos. Chem. Phys., 9, 635–665, https://doi.org/10.5194/acp-9-635-2009, 2009.

Yuan, Y., Zhao, X., Wang, S., and Wang, L: Atmospheric Oxidation of Furan and Methyl-Substituted Furans Initiated by Hydroxyl Radicals, J. Phys. Chem. A, 121, 9306-9319, 2017.

Zhou, L., Ravishankara, A. R., Brown, S. S., Idir, M., Zarzana, K. J., Daële, V., and Mellouki, A.: Kinetics of the Reactions of NO_3 Radical with Methacrylate Esters, J. Phys. Chem. A, 121, 4464-4474, 2017.